Discoveries

ORIGINAL RESEARCH COMMUNICATION

HJV and HFE Play Distinct Roles in Regulating Hepcidin

Qian Wu,[1,2,*] Hao Wang,[1,2,*] Peng An,[2,3] Yunlong Tao,[2] Jiali Deng,[1] Zhuzhen Zhang,[2]
Yuanyuan Shen,[2] Caiyong Chen,[4] Junxia Min,[3,5] and Fudi Wang[2,5,6]

Abstract

Aims: Hereditary hemochromatosis (HH) is an iron overload disease that is caused by mutations in *HFE*, *HJV*, and several other genes. However, whether HFE-HH and HJV-HH share a common pathway *via* hepcidin regulation is currently unclear. Recently, some HH patients have been reported to carry concurrent mutations in both the *HFE* and *HJV* genes. To dissect the roles and molecular mechanisms of HFE and/or HJV in the pathogenesis of HH, we studied $Hfe^{-/-}$, $Hjv^{-/-}$, and $Hfe^{-/-}Hjv^{-/-}$ double-knockout mouse models. *Results:* $Hfe^{-/-}Hjv^{-/-}$ mice developed iron overload in multiple organs at levels comparable to $Hjv^{-/-}$ mice. After an acute delivery of iron, the expression of hepcidin (*i.e.*, *Hamp1* mRNA) was increased in the livers of wild-type and $Hfe^{-/-}$ mice, but not in either $Hjv^{-/-}$ or $Hfe^{-/-}Hjv^{-/-}$ mice. Furthermore, iron-induced phosphorylation of Smad1/5/8 was not detected in the livers of $Hjv^{-/-}$ or $Hfe^{-/-}Hjv^{-/-}$ mice. *Innovation:* We generated and phenotypically characterized $Hfe^{-/-}Hjv^{-/-}$ double-knockout mice. In addition, because they faithfully phenocopy clinical HH patients, these mouse models are an invaluable tool for mechanistically dissecting how HFE and HJV regulate hepcidin expression. *Conclusions:* Based on our results, we conclude that HFE may depend on HJV for transferrin-dependent hepcidin regulation. The presence of residual hepcidin in the absence of HFE suggests either the presence of an unknown regulator (*e.g.*, TFR2) that is synergistic with HJV or that HJV is sufficient to maintain basal levels of hepcidin. *Antioxid. Redox Signal.* 22, 1325–1336.

Introduction

IRON IS AN ESSENTIAL element for normal cellular function. However, iron is also a pro-oxidant factor that causes oxidative stress by catalyzing a Fenton reaction, yielding reactive oxygen species. Iron overload-induced oxidative damage can cause cellular defects such as mitochondrial and DNA damage, lipid peroxidation, and protein modification, all of which subsequently cause damage to multiple organs, including the liver, heart, and pancreas of patients with hemochromatosis (18).

Iron metabolism has been studied extensively during the past decade. In particular, the hepcidin-ferroportin regulatory axis has been investigated in an attempt to understand how the body maintains iron homeostasis (2, 13, 16). Hepcidin was initially identified as an antimicrobial peptide that is secreted by the liver (20) and exerts negative effects on intestinal iron absorption and iron recycling in macrophages (25). Moreover, classic hereditary hemochromatosis (HH)—which is characterized by the progressive development of severe iron overload in multiple organs—can result directly from hepcidin deficiency (1, 6, 31).

Many proteins and pathways are involved in the regulation of hepcidin. For example, changes in transferrin saturation can cause conformational changes in HFE/TfR2 (transferrin receptor 2), which modulates hepcidin expression (12, 15, 33). Several bone morphogenetic protein (BMP) family members (including Bmp2, Bmp4, Bmp6, and Bmp9) can

[1]Key Laboratory of Nutrition and Metabolism, Institute for Nutritional Sciences, Shanghai Institutes for Biological Sciences, Chinese Academy of Sciences, University of the Chinese Academy of Sciences, Shanghai, China.
[2]Department of Nutrition, Research Center for Nutrition and Health, Institute of Nutrition and Food Safety, School of Public Health, School of Medicine, Zhejiang University, Hangzhou, China.
[3]The First Affiliated Hospital, Institute for Translational Medicine, School of Medicine, Zhejiang University, Hangzhou, China.
[4]College of Life Sciences, Zhejiang University, Hangzhou, China.
[5]Collaborative Innovation Center for Diagnosis and Treatment of Infectious Diseases, Zhejiang University, Hangzhou, China.
[6]School of Public Health, Zhengzhou University; Shandong Provincial Collaborative Innovation Center for Neurodegenerative Disorders, Qingdao University; Beijing Center of Food Nutrition and Human Health, China Agricultural University, Beijing, China.
*These two authors contributed equally to this article as first authors.

Innovation

For more than a decade, hepcidin has been studied as a potential molecule for preventing iron overload. However, although the proteins HJV and HFE are key modulators of hepcidin expression, whether these two proteins act *via* parallel or converging pathways remains unknown. We therefore generated $Hfe^{-/-}Hjv^{-/-}$ mice and found that these double-knockout mice develop an iron overload phenotype that is strikingly similar to $Hjv^{-/-}$ single-knockout mice. Importantly, the response of hepcidin to acute iron treatment was dominated by HJV (but not HFE), and the mitogen-activated protein kinase (MAPK)/ extracellular signal regulated kinase (Erk) pathway was not mainly involved in this process. These findings suggest that HJV is the key regulator of hepcidin and that HFE acts in an HJV-dependent manner.

upregulate hepcidin expression *via* the BMP/Smad pathway (3, 35). Moreover, inflammatory cytokines (*e.g.*, IL-6) and infectious stimuli can activate hepcidin *via* the IL-6/Stat3 pathway (4, 24, 36).

HFE plays a regulatory role in the hepcidin pathway (6, 41), and mutations in the *HFE* gene cause Type I HH (10). In addition, HFE-deficient mice develop an iron overload phenotype that is strikingly similar to Type I HH in patients (41), and a study by Schmidt *et al.* revealed that HFE positively modulates the expression of hepcidin (33). HFE interacts with transferrin receptor 1 (TfR1) and competes with the receptor's transferrin (Tf) binding site (23), thereby activating downstream signaling pathways, including the mitogen-activated protein kinase (MAPK) pathway. Because the MAPK pathway can crosstalk with the BMP/Smad pathway, this activation can upregulate hepcidin expression at the transcriptional level (15, 33).

HJV is another principal modulator of hepcidin expression, and mutations in the *HJV* gene cause Type II HH (27). Membrane-bound HJV binds to BMPs, thereby acting as a co-receptor along with the Bmp receptor (3). The expression of Bmp6 is positively correlated with iron content in the liver (19), and binding of Bmp6 to the Bmp receptor triggers Smad1/ 5/8 phosphorylation, thus upregulating hepcidin expression. *In vitro* studies have shown that HJV is required for activation of the BMP/Smad pathway (5, 26). Thus, HJV is considered a necessary component of the Bmp6/Smad pathway.

The relationship between HFE and HJV has long been debated. Studies suggest that HFE/TfR2 activates the MAPK pathway (28, 29), although the extent of the crosstalk between the MAPK and BMP/Smad pathways remains unclear. Recently, patients with mutations in both HFE and HJV have been reported (22), revealing the complexity of mutations and pathogenesis in HH patients. Understanding the roles played by HFE and HJV in regulating hepcidin will help unravel the genetic analyses and therapeutic diagnoses of patients with HH.

To address these issues, we characterized the phenotypes, hepcidin expression levels, and Smad phosphorylation levels in $Hfe^{-/-}$, $Hjv^{-/-}$ and $Hfe^{-/-}Hjv^{-/-}$ knockout mouse models. Interestingly, the $Hfe^{-/-}Hjv^{-/-}$ double-knockout mice developed the same iron overload phenotype as $Hjv^{-/-}$ single-knockout mice. Consistent with this finding, hepatic

hepcidin expression and Smad protein phosphorylation levels were similar between the $Hfe^{-/-}Hjv^{-/-}$ and $Hjv^{-/-}$ mice. Furthermore, an acute oral bolus of iron significantly increased hepcidin mRNA levels in the livers of $Hfe^{-/-}$ mice, but was without effect on the $Hfe^{-/-}Hjv^{-/-}$ and $Hjv^{-/-}$ mice. Based on these results, we hypothesize that HFE requires HJV to activate downstream signal transduction pathways.

Results

### Hfe knockout does not increase iron overload in Hjv$^{-/-}$ mice

Eight-week-old wild-type, $Hfe^{-/-}$, $Hjv^{-/-}$, and $Hfe^{-/-}Hjv^{-/-}$ mice (three to four mice per group) were sacrificed, and blood and tissue samples were collected for analysis. The serum iron (Fig. 1A) and transferrin saturation (Fig. 1B) levels were significantly elevated in all three knockout lines. The hepatic iron content (HIC) was higher in both the $Hjv^{-/-}$ and $Hfe^{-/-}Hjv^{-/-}$ mice compared with the $Hfe^{-/-}$ mice, with no difference between the $Hjv^{-/-}$ and $Hfe^{-/-}Hjv^{-/-}$ mice (Fig. 1C). This trend was observed in both males and females in each line, and we found no difference between male and female in $Hfe^{-/-}$, $Hjv^{-/-}$ and $Hfe^{-/-}Hjv^{-/-}$ mice with respect to iron parameters, except that HIC in female wild-type mice is higher than in male wild-type mice. Prussian blue staining of liver sections revealed iron overload in the hepatocytes of all three knockout lines, with the most intense staining in $Hjv^{-/-}$ and $Hfe^{-/-}Hjv^{-/-}$ hepatocytes (Fig. 1G).

To examine the roles of *Hjv* and *Hfe* in iron homeostasis at a younger age, we measured the serum and liver iron contents in 3-week-old wild-type and knockout mice. At this age, the serum iron and transferrin saturation levels did not differ significantly between the $Hjv^{-/-}$ and $Hfe^{-/-}Hjv^{-/-}$ mice (Fig. 1D, E). Similar to the 8-week-old mice, all three knockout lines had significant hepatic iron overload compared with wild-type mice, with both the $Hjv^{-/-}$ and $Hfe^{-/-}Hjv^{-/-}$ mice having higher hepatic iron overload than the $Hfe^{-/-}$ mice (Fig. 1F). We found no difference between males and females in $Hjv^{-/-}$ and $Hfe^{-/-}Hjv^{-/-}$ mice with respect to iron parameters.

Reduced hepcidin expression in Hfe$^{-/-}$, Hjv$^{-/-}$, and Hfe$^{-/-}$ Hjv$^{-/-}$ mice

Next, we used real-time polymerase chain reaction (PCR) to measure the basal hepatic expression levels of *Hamp1*, *Id1*, *Smad7*, and *Bmp6* in wild-type mice and all three knockout mouse lines of both genders. Compared with wild-type mice, all three knockout lines had significantly lower *Hamp1* expression; specifically, the *Hamp1* mRNA level in $Hfe^{-/-}$ mice was 35% of wild-type levels, and *Hamp1* mRNA levels in both $Hjv^{-/-}$ and $Hfe^{-/-}Hjv^{-/-}$ mice was < 2.5% of wild-type levels (Fig. 2A). There was no significant difference between the $Hjv^{-/-}$ and $Hfe^{-/-}Hjv^{-/-}$ mice with respect to *Hamp1* expression. Similarly, the expression levels of both *Id1* and *Smad7* were lower in the $Hjv^{-/-}$ and $Hfe^{-/-}Hjv^{-/-}$ compared with the wild-type and $Hfe^{-/-}$ mice, and there was no significance difference between the $Hjv^{-/-}$ and $Hfe^{-/-}Hjv^{-/-}$ mice (Fig. 2B, C). This trend was observed for both genders in every line. In general, *Hamp1* mRNA levels are higher in females than those in males in wild-type, $Hjv^{-/-}$, and $Hfe^{-/-}Hjv^{-/-}$ mice.

FIG. 1. Iron accumulates in $Hfe^{-/-}$, $Hjv^{-/-}$, and $Hfe^{-/-}Hjv^{-/-}$ double-knockout mice. (A) Serum iron, (B) transferrin saturation, and (C) hepatic non-heme iron levels were measured in 8-week-old WT (eight male, eight female), $Hfe^{-/-}$ (eight male, eight female), $Hjv^{-/-}$ (eight male, eight female), and $Hjv^{-/-}$ $Hfe^{-/-}$ (eight male, eight female) mice. (D) Serum iron, (E) transferrin saturation, and (F) hepatic non-heme iron levels were measured in 3-week-old WT (eight male, eight female), $Hfe^{-/-}$ (eight male, eight female), $Hjv^{-/-}$ (eight male, eight female), and $Hjv^{-/-}$ $Hfe^{-/-}$ (eight male, eight female) mice. In this and subsequent figures, the data are presented as mean ± standard error of the mean. Statistical analysis in (C) and (F) was carried out by using log-transformed values to meet homogenous variances, and then all data were compared using an ANOVA with Tukey's test. Labeled without a common *letter* (a, b, c, or d) indicates significant difference among tested groups ($p < 0.05$). (G) Liver sections were stained with Perls Prussian blue. The scale bar represents 100 μm. ANOVA, analysis of variance; WT, wild-type.
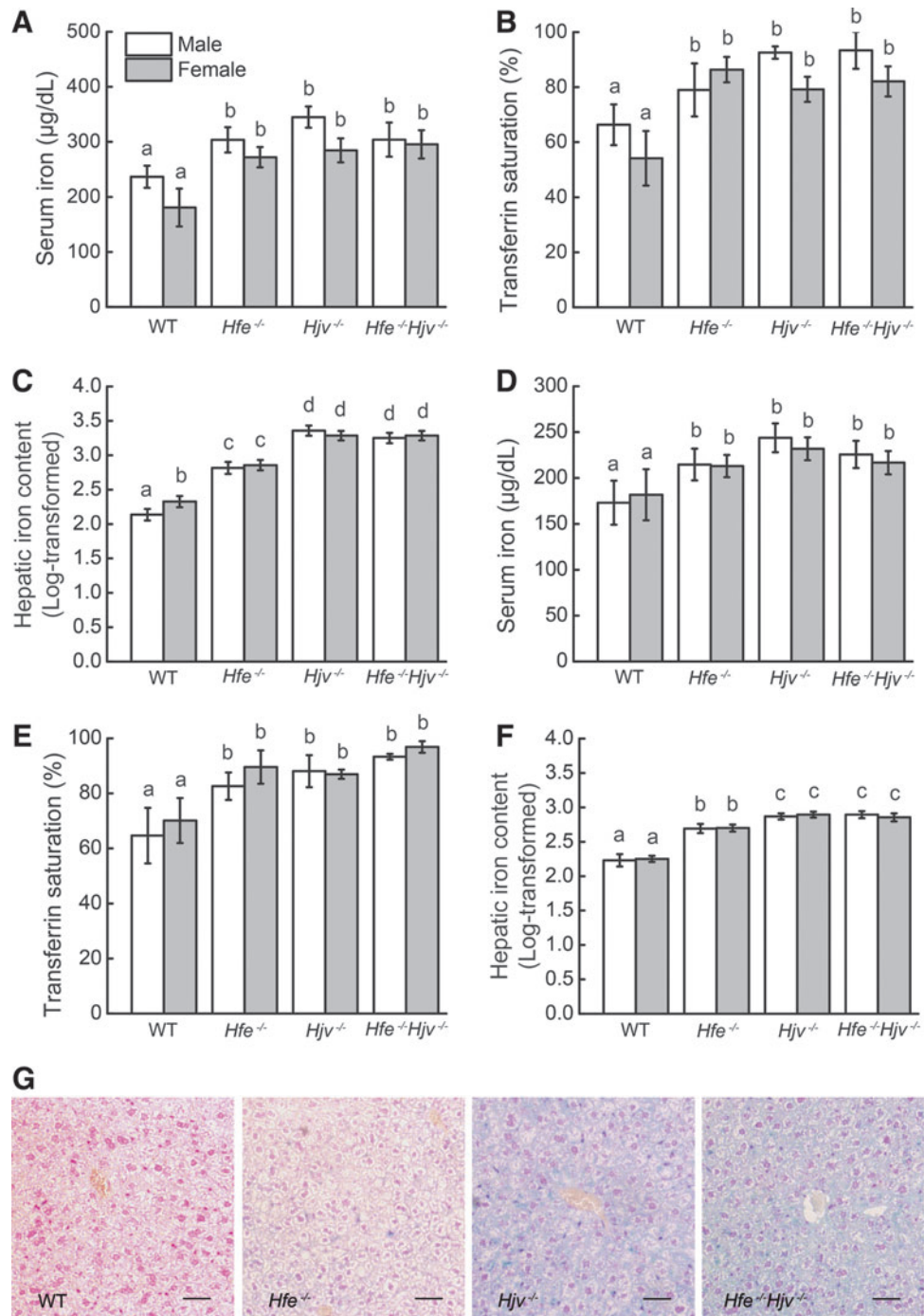
Compared with the wild-type and $Hfe^{-/-}$ mice, the hepatic expression of *Bmp6* was significantly higher in both the $Hjv^{-/-}$ and $Hfe^{-/-}Hjv^{-/-}$ mice (Fig. 2D). *Bmp6* expression was positively correlated to *Hamp1* (and other Smad1/5/8 targeting genes, including *Id1* and *Smad7*) levels when the Bmp/Smad pathway was intact; thus, we used the ratios of *Hamp1/Bmp6*, *Id1/Bmp6*, and *Smad7/Bmp6* expression to assess the integrity of the Bmp/Smad pathway. We next measured the ratio of *Hamp1/Bmp6* mRNA levels in all mouse lines (Fig. 2E). *Hamp1/Bmp6* ratio was lower in all three knockout mice when compared with wild-type mice; the ratios in the $Hjv^{-/-}$ and $Hfe^{-/-}Hjv^{-/-}$ mice were even

lower compared with the $Hfe^{-/-}$ mice, although there was no significant difference between the $Hjv^{-/-}$ and $Hfe^{-/-}Hjv^{-/-}$ mice. In addition, *Hamp1/Bmp6* ratio was higher in females than in males in both $Hjv^{-/-}$ and $Hfe^{-/-}Hjv^{-/-}$ mice but not in wild-type or $Hfe^{-/-}$ mice. The ratios of *Id1/Bmp6* mRNA and *Smad7/Bmp6* mRNA (Fig. 2F, G) showed similar pattern as the ratio of *Hamp1/Bmp6* in all mouse lines. We also measured the levels of phosphorylated Smad1/5/8 (P-Smad1/5/8) in each gender using Western blot analysis. In comparison to WT mice, all three knockout lines showed attenuated P-Smad1/5/8. When three knockout lines were compared, we found that P-Smad1/5/8 levels in the $Hjv^{-/-}$ and $Hfe^{-/-}$
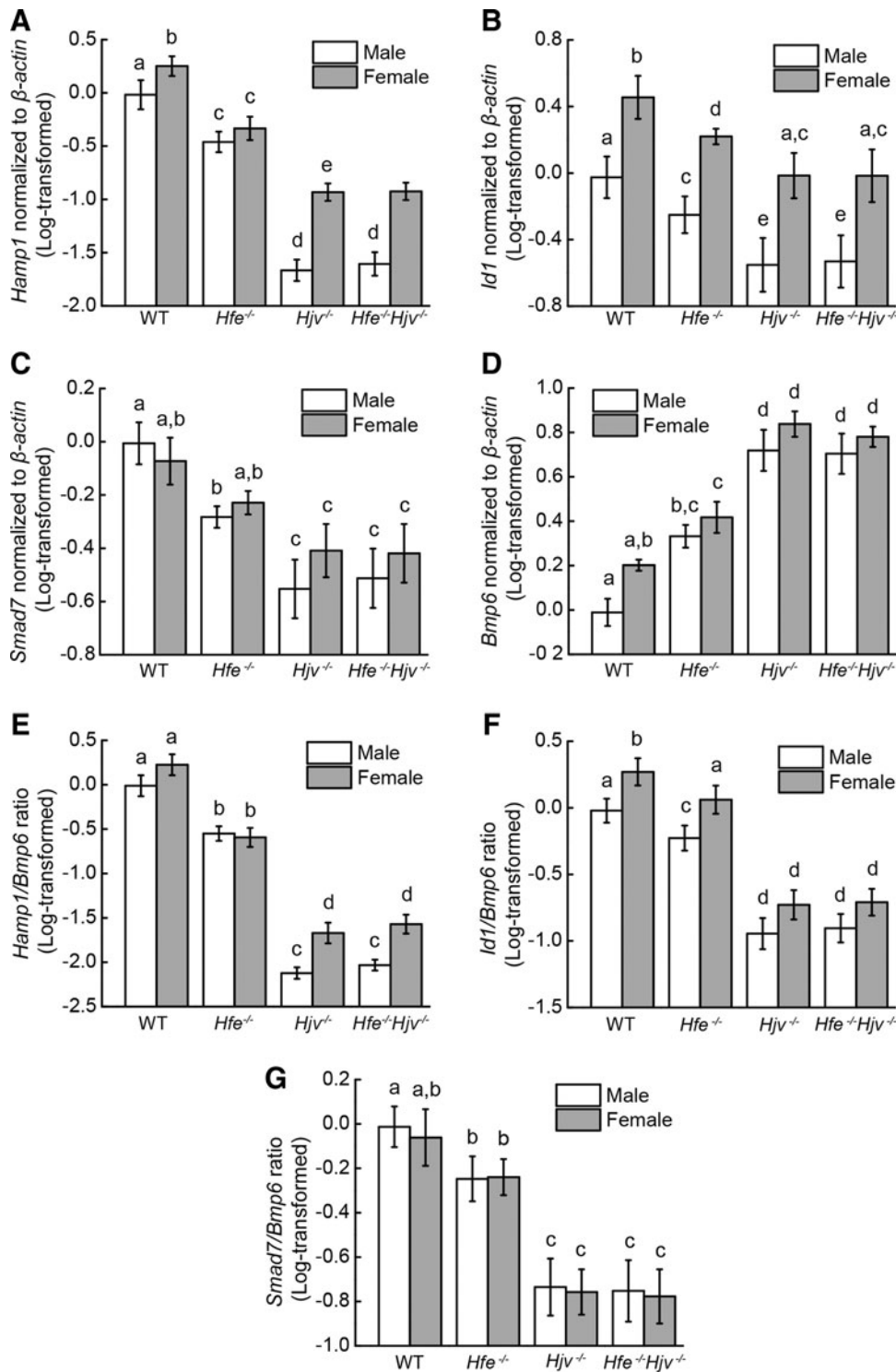
FIG. 2. *Hamp1*, *Id1*, and *Smad7* expression, and Bmp6/Smad signaling in *Hfe*$^{-/-}$, *Hjv*$^{-/-}$, and *Hfe*$^{-/-}$*Hjv*$^{-/-}$ double-knockout mice. Hepatic (**A**) *Hamp1*, (**B**) *Id1*, (**C**) *Smad7*, and (**D**) *Bmp6* mRNA levels were measured in 8-week-old wild-type (eight male, eight female), *Hfe*$^{-/-}$ (eight male, eight female), *Hjv*$^{-/-}$ (eight male, eight female), and *Hjv*$^{-/-}$*Hfe*$^{-/-}$ (eight male, eight female) mice that were fed a standard diet; the mRNA levels were normalized to β-*actin* mRNA and are expressed relative to the mean value of wild-type males. The (**E**) *Hamp1/Bmp6*, (**F**) *Id1/Bmp6*, and (**G**) *Smad7/Bmp6* ratios were calculated for each mouse and relative to the mean value of wild-type males. Statistical analyses were conducted by using log-transformed values to meet homogenous variances, and then all data were compared using an ANOVA with Tukey's test. Labeled without a common *letter* (a, b, c, d, or e) indicates significant difference among tested groups ($p < 0.05$).

Hjv$^{-/-}$ mice are significantly lower than in the *Hfe*$^{-/-}$ mice. Notably, there was no apparent difference between *Hjv*$^{-/-}$ and *Hfe*$^{-/-}$*Hjv*$^{-/-}$ mice (Fig. 3A, B).

Acute iron delivery alters hepcidin expression in an Hjv-dependent manner

We next delivered an acute bolus of iron to the mice and measured the effect on hepcidin expression. All three

knockout lines were first fed an iron-deficient diet for 3–5 weeks, and the wild-type mice were fed a standard diet containing normal levels of iron to achieve comparable iron levels between wild-type mice and knockout mice. All four groups were then given a single dose of iron by oral gavage to perturb the serum iron levels without affecting HIC. Four hours after treatment, the mice were sacrificed, and blood and tissue samples were collected for analysis. In each line (including the wild-type mice), the single delivery of iron
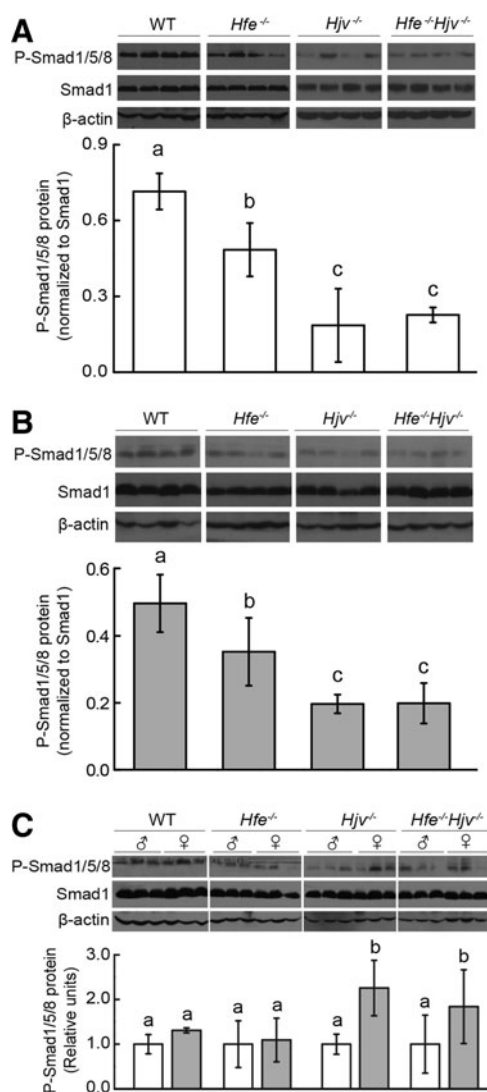
FIG. 3. Hepatic P-Smad1/5/8 levels in both male and female $Hfe^{-/-}$, $Hjv^{-/-}$, and $Hfe^{-/-}Hjv^{-/-}$ double-knockout mice. Hepatic Smad1 and P-Smad1/5/8 levels in (**A**) male, (**B**) female, and (**C**) both genders were measured using Western blot analysis. The bands were quantified, and P-Smad1/5/8 levels were normalized to Smad1 levels. All data were compared using an ANOVA with Tukey's test. Labeled without a common *letter* (a, b, or c) indicates significant difference among tested groups ($p < 0.05$).
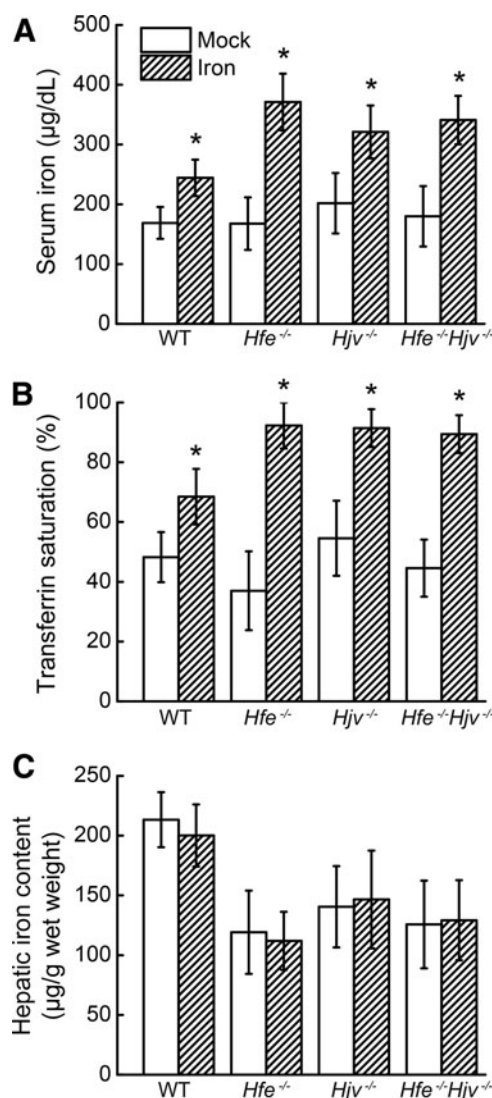

FIG. 4. Acute iron treatment alters serum iron levels and transferrin saturation but not hepatic iron content in wild-type, $Hfe^{-/-}$, $Hjv^{-/-}$, or $Hfe^{-/-}Hjv^{-/-}$ mice. (A) Serum iron levels, (**B**) transferrin saturation, and (**C**) hepatic iron content were measured in the mice shown in Figure 3, which received mock (*white bars*) or iron (*italic bars*) treatment by oral gavage. The data were compared using the Student's *t*-test; *$p < 0.05$ *versus* the respective mock group.

significantly elevated the serum iron and transferrin saturation levels (Fig. 4A, B). Furthermore, HIC (Fig. 4C) and hepatic *Bmp6* mRNA expression (Fig. 5A) were similar between the iron-treated and mock-treated groups. Interestingly, both the wild-type and $Hfe^{-/-}$ mice had significantly elevated hepatic *Hamp1* mRNA expression ($\sim$2-fold higher than the mock-treated mice); in contrast, hepatic *Hamp1* mRNA levels were not affected by acute iron treatment in either the $Hjv^{-/-}$ or $Hfe^{-/-}Hjv^{-/-}$ mice (Fig. 5B). Similar results were obtained with respect to hepatic *Id1* and *Smad7* mRNA levels (Fig. 5C, D). *Hamp1* expression in the three knockout lines that were fed an iron-deficient diet did not differ; in contrast, the *Hamp1/Bmp6* ratios were similar to the mice that were fed a normal diet (Fig. 5E, F). Hepatic P-

Smad1/5/8 levels were also significantly elevated in the iron-treated wild-type and $Hfe^{-/-}$ mice, whereas the P-Smad1/5/8 levels were not affected by iron treatment in either the $Hjv^{-/-}$ or $Hfe^{-/-}Hjv^{-/-}$ mice (Fig. 5G). These results were consistent in both genders.

Crosstalk between the MAPK/Erk and Bmp/Smad pathways upstream of hepcidin expression

Under basal iron conditions, no significant difference in P-Erk1/2 levels was observed for either gender between the four lines (Fig. 6A, B). After acute iron treatment, no significant change in hepatic phosphorylated extracellular signal regulated kinase (P-Erk) levels was observed in either the wild-type mice or any of the three knockout lines (data not shown).
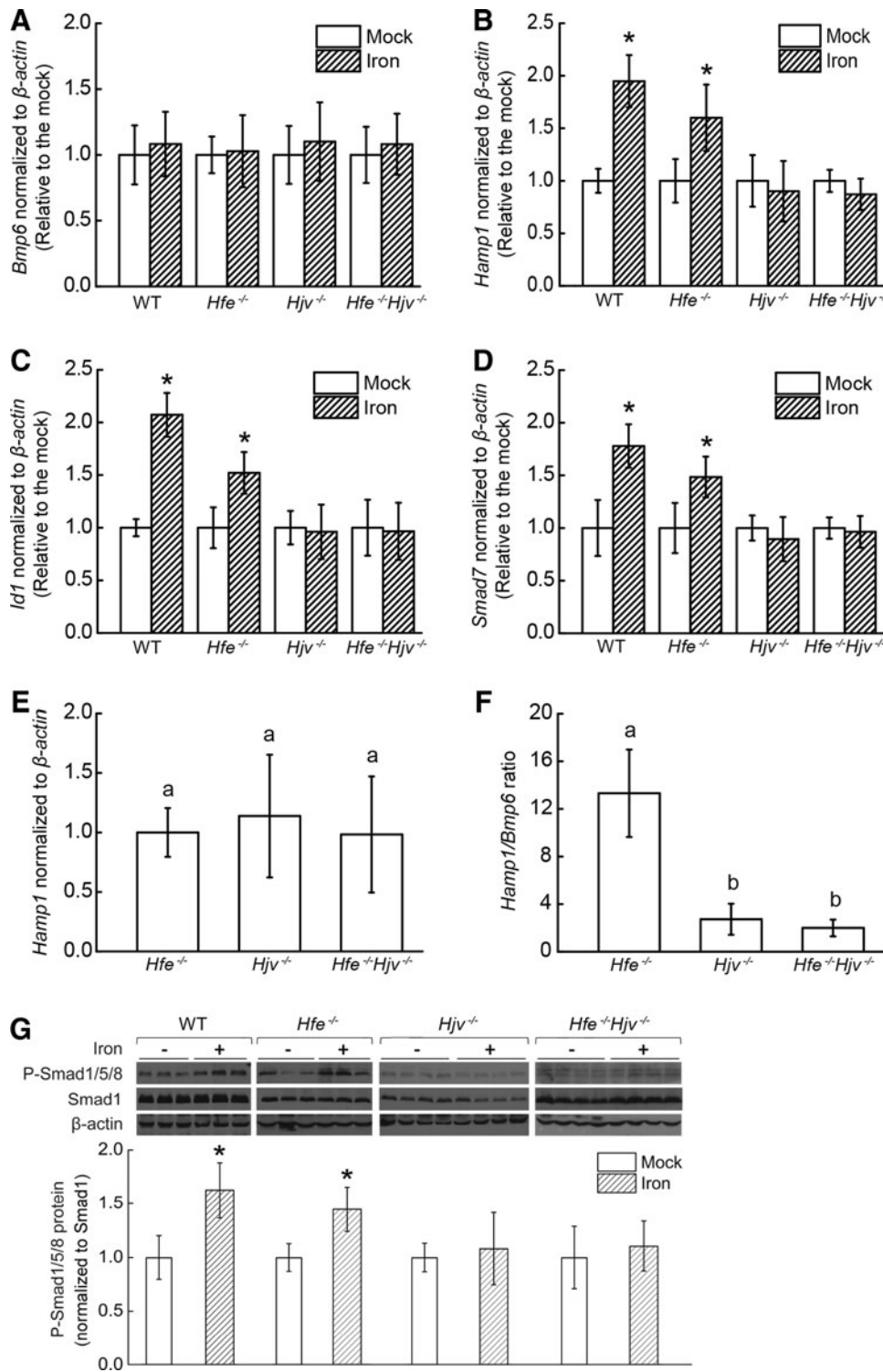
FIG. 5. $Hjv^{-/-}$ and $Hjv^{-/-}$ $Hfe^{-/-}$ mice have an attenuated hepcidin response to acute iron treatment. Eight-week-old wild-type, $Hfe^{-/-}$, $Hjv^{-/-}$, and $Hjv^{-/-}$ $Hfe^{-/-}$ mice were given $FeCl_3$ ("Iron"; $n=8$ mice/group) or distilled water ("Mock"; $n=8$ mice/group) by oral gavage; after 4 h, (A) Bmp6, (B) Hamp1, (C) Id1, (D) Smad7 mRNA, and (G) P-Smad1/5/8 levels were measured. Hepatic (E) Hamp1 mRNA levels in $Hfe^{-/-}$, $Hjv^{-/-}$, and $Hfe^{-/-}$ $Hjv^{-/-}$ mice that were fed an iron-deficient diet were detected, and (F) the hepatic Hamp1/Bmp6 ratio was calculated for each mouse. Hepatic Bmp6, Hamp1, Id1, and Smad7 mRNA was normalized to β-actin and expressed relative to the mean value of each genotype's respective mock group. Hepatic P-Smad1/5/8 levels were quantified, normalized to Smad1, and expressed relative to the mean value of each genotype's respective mock group. The data in (A–D) and (G) were analyzed using the Student's t-test; *$p < 0.05$ versus the respective mock group. The data in (E, F) were compared using an ANOVA with Tukey's test. Labeled without a common letter (a, b) indicates significant difference among tested groups ($p < 0.05$).

Next, primary hepatocytes were isolated from all four mouse lines and treated with both serum and holotransferrin for 0, 5, or 15 min, after which P-Erk levels were measured using Western blot analysis. As shown in Figure 6C, Erk phosphorylation levels peaked at 5 min in all four lines, but only in those of the $Hjv^{-/-}$, and the double knockout mice returned to baseline at a 15-min time point when treated with serum + holotransferrin. In the presence of the MAPK inhibitor U0-126, Erk1/2 phosphorylation was completely blocked at the 5-min time point (Fig. 6C). Finally, Hamp1 expression was significantly upregulated in wild-type and $Hfe^{-/-}$ hepatocytes after treatment with holotransferrin, but was not activated in the $Hjv^{-/-}$ or $Hfe^{-/-} Hjv^{-/-}$ hepatocytes (Fig. 6D).

Discussion

In this study, we generated $Hfe^{-/-} Hjv^{-/-}$ mice and compared these double-knockout mice with wild-type and
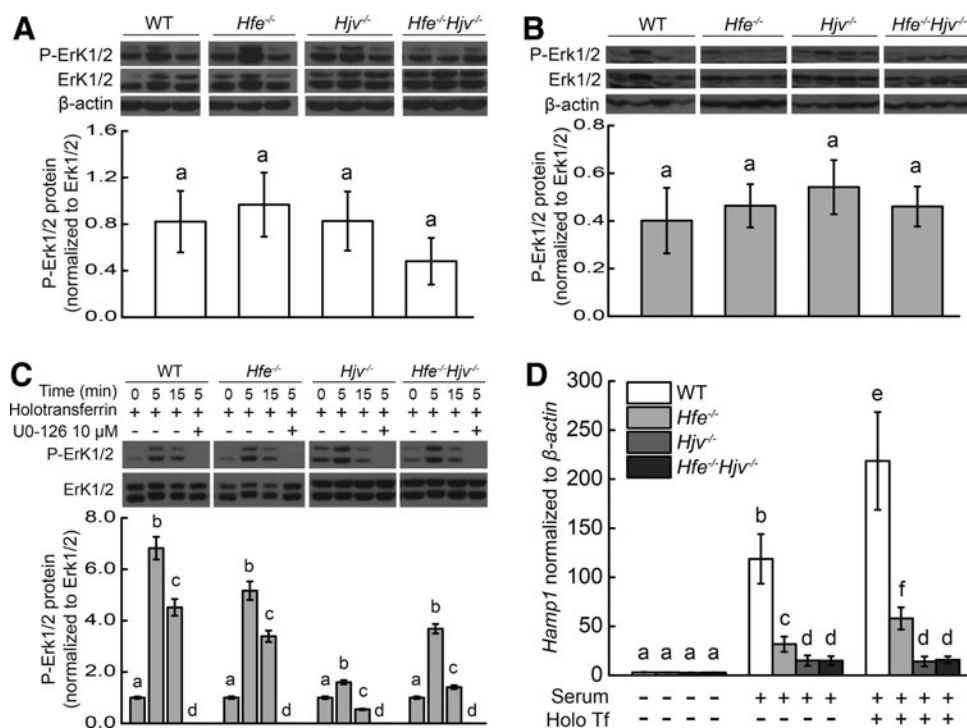
FIG. 6. **The MAPK/Erk pathway is partial functional in $Hfe^{-/-}$, $Hjv^{-/-}$, and $Hfe^{-/-}Hjv^{-/-}$ mice.** Basal P-Erk1/2 levels were measured in (**A**) male and (**B**) female wild-type, $Hfe^{-/-}$, $Hjv^{-/-}$, and $Hfe^{-/-}Hjv^{-/-}$ mice and normalized to total Erk1/2 protein levels. Primary hepatocytes were isolated from the indicated mouse lines, then treated with serum and holotransferrin in the absence or presence of $10\,\mu M$ U0-126 for the indicated times. (**C**) P-Erk1/2 was then measured using Western blot analysis, and (**D**) *Hamp1* mRNA was measured using real-time polymerase chain reaction. The bands were quantified, and P-Erk1/2 levels were normalized to Erk1/2 levels. The primary culture experiments were repeated three independent times. Statistical analyses were carried out by using log-transformed values to meet homogenous variances, and then all data were compared using an ANOVA with Tukey's test. Labeled without a common *letter* (a, b, c, d, e, or f) indicates significant difference among tested groups ($p < 0.05$). Erk, extracellular signal regulated kinase; MAPK, mitogen-activated protein kinase; P-Erk, phosphorylated Erk.

single-knockout $Hfe^{-/-}$ and $Hjv^{-/-}$ mice to identify the unique and/or synergistic roles that HFE and HJV play in regulating hepcidin. We found that both 3- and 8-week-old double-knockout mice develop an iron-related phenotype that is similar to $Hjv^{-/-}$ single-knockout mice (Fig. 1). These results were supported by our mRNA and protein level analyses, indicating that an additional deletion of HFE expression does not exacerbate the iron accumulation and hepcidin deficiency caused by the loss of HJV alone (Figs. 2 and 3). To evaluate the role of HFE and HJV in the hepcidin regulation pathway during acute changes in iron status, we fed these knockout mouse lines an iron-deficient diet to induce iron levels that were similar to wild-type levels and then acutely perturbed serum iron levels with a single oral treatment of iron. We then compared *Hamp1* mRNA and P-Smad1/5/8 levels between the iron-treated and mock-treated groups. Interestingly, although iron treatment significantly increased *Hamp1* expression in the wild-type and $Hfe^{-/-}$ mice, iron treatment had no effect on the $Hjv^{-/-}$ or $Hfe^{-/-}Hjv^{-/-}$ mice (Fig. 5). Thus, these results suggest that Hjv elicits a stronger response to changes in serum iron levels than Hfe.

The basal iron parameters in the four mouse lines indicated differing degrees of iron homeostatic imbalance. To explore the underlying mechanisms, we measured *Hamp1* expression and the downstream signaling pathways in the liver. *Hamp1* expression was markedly reduced in the double-knockout mice to

a level similar to the $Hjv^{-/-}$ mice. In contrast, although *Hamp1* expression was reduced in the $Hfe^{-/-}$ mice, the effect was significantly weaker than in the $Hjv^{-/-}$ and $Hfe^{-/-}Hjv^{-/-}$ mice (Fig. 2A), indicating that this pathway is only partially impaired in $Hfe^{-/-}$ mice, consistent with a previous report (1). Furthermore, the different *Hamp1* expression levels among these lines are consistent with their differing iron statuses, and the hepatic P-Smad1/5/8 levels support these results (Fig. 3A, B). Thus, disrupting basal hepcidin expression causes iron accumulation in the knockout mice. Recently, digenic inheritance of mutations in both *HFE* and *HJV* in patients was reported to cause juvenile hemochromatosis with a phenotype similar to patients with a single (monogenic inherited) *HJV* mutation (22), which supports our findings in $Hfe^{-/-}Hjv^{-/-}$ mice.

Gender is an important modifying factor in iron homeostasis. For example, HFE-HH hemochromatosis has higher penetrance in men than in women, mostly likely because of the physiological iron loss through menstruation and pregnancy (14). However, penetrance in HJV-HH was similar in women and men. In our study, we found there are no differences in measured iron parameters between female and male $Hjv^{-/-}$ or $Hfe^{-/-}Hjv^{-/-}$ mice. Interestingly, we observed that hepatic *Hamp1* expression levels in female mice were higher than those in male mouse lines, and higher P-Smad1/5/8 levels were found in females than in males in terms of $Hjv^{-/-}$ and $Hfe^{-/-}Hjv^{-/-}$ lines (Fig. 3C), in which

similar phenomena were also indicated in previous reports (21). Finally, the mechanisms that underlie iron metabolism differ between mice and humans (2). Therefore, the gender-related effect on the penetrance of hemochromatosis in humans with combined HFE and HJV mutations might not correlate directly with our animal studies.

Previous reports suggest that HFE and HJV regulate hepcidin expression *via* distinct pathways (5, 15, 17, 23, 26, 32, 33). However, deleting both genes did not exacerbate the phenotype. Knocking out HJV alone effectively impairs the BMP/Smad pathway, which may lead to reduced hepcidin expression. However, whether this reduction in hepcidin expression reaches a very low level in $Hjv^{-/-}$ mice is unclear. Studies have shown that hepcidin expression is still detectable in $Hjv^{-/-}$ mice (17), which is in agreement with our findings. Moreover, inflammatory stimuli can modulate hepcidin expression in $Hjv^{-/-}$ mice (17), which suggests that deleting HJV does not block the entire hepcidin pathway, but may block only the BMP/Smad pathway. In addition, when $Hjv^{-/-}$ mice were fed an iron-rich diet (30), hepcidin expression still responded to iron loading, indicating that the mechanism by which iron modulates hepcidin is partially functional even in the absence of HJV. On the other hand, HJV might play an indispensable role in HFE-dependent signaling. A recent study showed that HJV interacts with HFE and the TfR2 (9); thus, deleting HJV may abrogate both Bmp and HFE/TfR2 signaling, thereby masking the effect of

also deleting HFE in the $Hfe^{-/-}Hjv^{-/-}$ double-knockout mice. Therefore, further studies are needed to determine whether the HFE/TfR2 signaling complex still responds to changes in transferrin in our knockout mice.

We also examined Hfe's role in our knockout mice models, as HFE was previously considered an iron sensor that contributes to hepcidin regulation. Given that our knockout mouse models develop iron overload (16, 38), it is conceivable that the basal iron status of these mice might overcome the changes in iron caused by acute iron treatment. Thus, we accounted for this possibility by inducing dietary iron deficiency (DID) in each knockout line. After consuming an iron-deficient diet for 5 weeks, the serum iron, transferrin saturation, and liver iron levels in the knockout mice were similar to—or lower than—the levels in wild-type mice that were fed a standard diet. Acutely treating the mice with oral iron had no effect on liver iron content in any of the mouse lines (Fig. 4C); therefore, we only considered the transferrin-dependent pathway in our treatment. Accordingly, we assessed the effect of acutely delivering iron to DID mice by oral gavage (8), and we found that transferrin saturation dramatically increased in all iron-treated groups (Fig. 4B). We then measured hepatic expression in the iron-treated and mock-treated groups. In the wild-type group, both *Hamp1* expression and Smad1/5/8 phosphorylation were significantly increased, consistent with previous reports (8). Similarly, we also observed a significant increase in hepatic
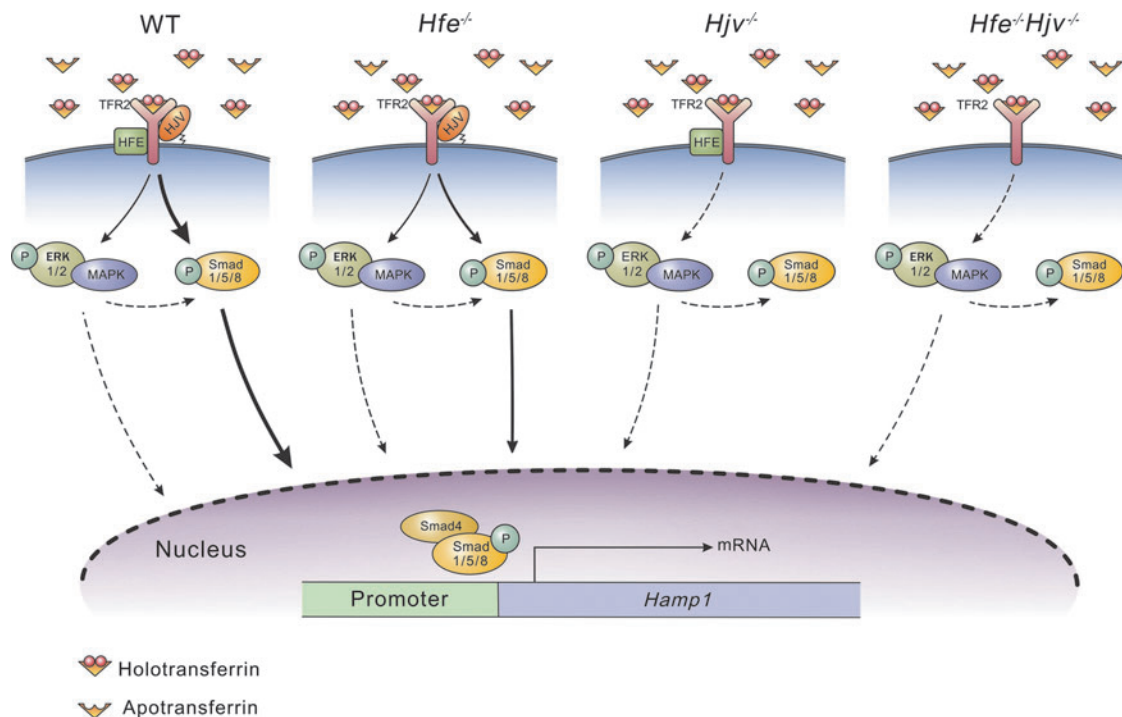

FIG. 7.   Proposed model illustrating the relationship between HJV and HFE in regulating hepcidin expression in response to an acute increase in serum iron levels. Elevated serum iron triggers the phosphorylation of Smad1/5/8, which then binds to Smad4. The P-Smad1/5/8-Smad4 complex then translocates to the nucleus, where it drives the expression of hepcidin (*via* the *Hamp1* gene). HFE and TFR2 can sense an increase serum iron and transduce a signal that, ultimately, leads to the phosphorylation of Smad1/5/8. Our results suggest that HJV predominantly controls the phosphorylation of Smad1/5/8, and HFE activity is dependent on HJV. In our mouse models of hereditary hemochromatosis (*i.e.*, the $Hfe^{-/-}$, $Hjv^{-/-}$, and $Hjv^{-/-}Hfe^{-/-}$ mice), HFE deletion partially reduces P-Smad1/5/8 levels and hepcidin expression on stimulation with holotransferrin; in contrast, deleting HJV blocks this pathway completely. Moreover, crosstalk between the Erk/MAPK and Bmp/Smad pathways was previously believed to be necessary for holotransferrin-induced hepcidin expression (*dashed arrows*).

Hamp1 expression and P-Smad1/5/8 levels in the iron-treated $Hfe^{-/-}$ DID group (Fig. 5B, G). Moreover, a similar fold change in *Hamp1* expression was induced by culturing primary $Hfe^{-/-}$ and wild-type hepatocytes in holo-transferrin (29), whereas *Hamp1* induction by transferrin was abrogated in primary hepatocytes isolated from $Hjv^{-/-}$ and double-knockout mice (data not shown). These results suggest that transferrin-dependent signaling is partially preserved in the absence of HFE and is blocked completely by HJV deletion (Fig. 7). An unknown component (*e.g.*, TfR2)—or perhaps HJV itself—would be sufficient for basal transferrin-induced hepcidin expression.

The Erk pathway has been reported to play a role in transferrin-mediated signaling (29). However, we have not observed any significant difference of Erk1/2 phosphorylation in four tested mouse lines (Fig. 6A, B). We found P-Erk1/2 levels peaked at 5-min time point in holotransferrin-treated primary cultured hepatocytes in all four mouse lines (Fig. 6C). These observations indicate that the holotransferrin-induced activation of MAPK-Erk pathway might not be the main downstream pathways of either HFE or HJV, since the pathway can be activated even without either HFE or HJV. To avoid any potential artifacts due to transferrin, cytokines, and/or iron in the serum, we used serum-free cell culture medium as a control. As previously reported, P-Erk1/2 levels in serum-treated hepatocytes were also increased but weaker than holotransferrin+serum-treated hepatocytes (29). Nevertheless, this previous study also reported that an MEK inhibitor reduced Smad1/5/8 phosphorylation (29). Thus, the activation of MAPK might occur *via* another branch of the transferrin-TfR2 signaling pathway.

In this model (Fig. 7), when iron enters the circulation, apo-transferrin binds to ferric ions, creating holotransferrin. Holotransferrin then interacts with HFE/TFR2 (and possibly with HJV as well), triggering the phosphorylation of MAPK/Erk and Smad1/5/8. Our experiments show that MAPK/Erk might not play a key regulatory role in *Hamp1* expression, whereas P-Smad1/5/8 forms a complex with Smad4, translocates to the nucleus, and drives *Hamp1* transcription. In the *Hfe*-knockout line (depicted in the second model), the holotransferrin-induced signal remains less changed; however, because of the loss of HFE, the P-Smad1/5/8 signal is considerably weakened, and as a result, *Hamp1* expression in $Hfe^{-/-}$ mice is lower than wild-type expression. In the *Hjv*-knockout line (depicted in the third model), the holotransferrin signal cannot reach downstream signaling events; thus, even in the presence of HFE, *Hamp1* expression cannot proceed normally. This finding that transferrin-dependent signaling is absent in $Hjv^{-/-}$ mice underscores the importance of HJV in transferrin-dependent signaling. Finally, the HFE/HJV double-knockout mice (depicted in the fourth model) have similar signaling properties as the HJV single-knockout mice.

In summary, our findings add to our current knowledge with respect to the relationship between HFE and HJV. Although additional studies are warranted, our *in vivo* studies suggest that HJV is a key regulator that is necessary for HFE to increase hepcidin expression.

Materials and Methods

Animals

$Hfe^{-/-}$ mice and $Hjv^{-/-}$ mice were kindly provided by Dr. Nancy C. Andrews (11, 17). Both strains were maintained on a 129/SvEvTac background. $Hfe^{-/-} Hjv^{-/-}$ mice were generated by crossing the $Hfe^{-/-}$ and $Hjv^{-/-}$ mice. Unless stated otherwise, the mice were fed a standard rodent laboratory diet (containing 232 mg iron/kg) obtained from SLRC Laboratory Animal Co., Ltd. All experimental protocols were approved by the Institutional Animal Care and Use Committee of the Institute for Nutritional Sciences, Chinese Academy of Sciences.

Serum iron and tissue non-heme iron measurements

Serum iron and tissue non-heme iron were measured as previously described (34, 39).

Tissue iron staining

Tissue iron was detected in Bouin's solution-fixed liver and spleen sections using Perls Prussian blue staining. Slides were viewed using an Olympus IX51 microscope, and images were captured using an Olympus DP70 digital camera (37).

Induction of a DID model and acute iron administration

Three-week-old $Hfe^{-/-}$ mice were fed a standard diet for 2 weeks, after which they were fed an iron-deficient diet for 3 weeks. $Hjv^{-/-}$ and $Hfe^{-/-} Hjv^{-/-}$ mice were fed an iron-deficient diet for 5 weeks starting when they were weaned. The iron-deficient diet (containing 0.9 mg iron/kg) was the egg white-based AIN-76A-diet (Research Diets) (40). The DID mice and control diet-fed mice then received either 2 mg of elemental iron per kg body weight in the form of iron sulfate (Sigma) in 200 μl distilled water (iron-treated groups) or 200 μl distilled water alone (mock groups) by oral gavage; the mice were sacrificed 4 h after gavage, and serum and tissue samples were collected for analysis.

Primary hepatocyte culture and treatment

Hepatocytes were isolated from 8-week-old male wild-type (129/SvEvTac), $Hfe^{-/-}$, $Hjv^{-/-}$, and $Hfe^{-/-} Hjv^{-/-}$ mice using the collagenase isolation method as previously described (38). Hepatocytes were seeded in six-well plates at 1×10^6 cells per well. After the cells attached to the surface,

TABLE 1. SEQUENCES OF OLIGONUCLEOTIDE PRIMERS USED FOR REAL-TIME POLYMERASE CHAIN REACTION

Gene	Forward primer	Reverse primer
Actin	5′-AAA TCG TGC GTG ACA TCA AAG A-3′	5′-GCC ATC TCC TGC TCG AAG TC-3′
Hamp1	5′-GCA CCA CCT ATC TCC ATC AAC A-3′	5′-TTC TTC CCC GTG CAA AGG-3′
Id1	5′-CGC AGC CAC CGG ACT CT-3′	5′-AAC CCC CTC CCC AAA GTC T-3′
Smad7	5′-TTC GGA CAA CAA GAG TCA GC-3′	5′-GGT AAC TGC TGC GGT TGT AA-3′
Bmp6	5′-ATG GCA GGA CTG GAT CAT TGC-3′	5′-CCA TCA CAG TAG TTG GCA GCG-3′

the media was changed to fresh serum-free M199 media, and the cells were incubated for 42 h. Hepatocytes were then incubated with fresh media containing no serum (control), 10% fetal calf serum, 30 μM human holotransferrin (Sigma), or both 10% fetal calf serum and 30 μM human holotransferrin. Where indicated, the Erk inhibitor U0-126 (Cell Signaling) was added to a final concentration of 10 μM 1 h before the serum and/or holotransferrin treatment.

Real-time PCR analysis

Total RNA was isolated from the liver using Trizol (Invitrogen). Primer pairs were then used to detect iron-related mRNA transcripts (Table 1). Real-time PCR was performed using the two-step quantitative RT-PCR method as previously described (7), and target gene expression was normalized to β-*actin* mRNA levels.

Western blot analysis

Samples were prepared and analyzed using Western blot as previously described (39). Anti-phospho-Smad1/5/8 (1:1000; Cell Signaling), anti-Smad1 (1:1000; Cell Signaling), anti-phospho-Erk1/2 (1:1000; Cell Signaling), anti-Erk1/2 (1:1000; Cell Signaling), anti-TfR1 (1:500), and anti-β-actin (1:2000; Sigma) were used as the primary antibodies.

Statistical analysis

All summary data are expressed as the mean ± standard error of the mean ($n = 8$–10 mice/group). To compare multiple groups (*i.e.*, >2 groups), we first used Bartlett's test to check the homogeneity of variance. For multiple groups with unequal variance, the data were log$_{10}$-transformed to meet the assumption of homogeneity of variance, and then an analysis of variance (ANOVA) was performed, followed by Tukey's *post hoc* test. To compare two groups, differences were analyzed using the Student's *t*-test, and differences were considered statistically significant when $p < 0.05$. All statistical analyses were performed using the R software package.

Acknowledgments

Author Disclosure Statement

References

1. Ahmad KA, Ahmann JR, Migas MC, Waheed A, Britton RS, Bacon BR, Sly WS, and Fleming RE. Decreased liver hepcidin expression in the Hfe knockout mouse. *Blood Cells Mol Dis* 29: 361–366, 2002.

2. Andrews NC. Forging a field: the golden age of iron biology. *Blood* 112: 219–230, 2008.

3. Andriopoulos B, Jr., Corradini E, Xia Y, Faasse SA, Chen S, Grgurevic L, Knutson MD, Pietrangelo A, Vukicevic S, Lin HY, and Babitt JL. BMP6 is a key endogenous regulator of hepcidin expression and iron metabolism. *Nat Genet* 41: 482–487, 2009.

4. Armitage AE, Eddowes LA, Gileadi U, Cole S, Spottiswoode N, Selvakumar TA, Ho LP, Townsend AR, and Drakesmith H. Hepcidin regulation by innate immune and infectious stimuli. *Blood* 118: 4129–4139, 2011.

5. Babitt JL, Huang FW, Wrighting DM, Xia Y, Sidis Y, Samad TA, Campagna JA, Chung RT, Schneyer AL, Woolf CJ, Andrews NC, and Lin HY. Bone morphogenetic protein signaling by hemojuvelin regulates hepcidin expression. *Nat Genet* 38: 531–539, 2006.

6. Bridle KR, Frazer DM, Wilkins SJ, Dixon JL, Purdie DM, Crawford DH, Subramaniam VN, Powell LW, Anderson GJ, and Ramm GA. Disrupted hepcidin regulation in HFE-associated haemochromatosis and the liver as a regulator of body iron homoeostasis. *Lancet* 361: 669–673, 2003.

7. Bustin SA, Benes V, Garson JA, Hellemans J, Huggett J, Kubista M, Mueller R, Nolan T, Pfaffl MW, Shipley GL, Vandesompele J, and Wittwer CT. The MIQE guidelines: minimum information for publication of quantitative real-time PCR experiments. *Clin Chem* 55: 611–622, 2009.

8. Corradini E, Meynard D, Wu Q, Chen S, Ventura P, Pietrangelo A, and Babitt JL. Serum and liver iron differently regulate the bone morphogenetic protein 6 (BMP6)-SMAD signaling pathway in mice. *Hepatology* 54: 273–284, 2011.

9. D'Alessio F, Hentze MW, and Muckenthaler MU. The hemochromatosis proteins hfe, tfr2 and hjv form a membrane-associated protein complex for hepcidin regulation. *J Hepatol* 57: 1052, 2012.

10. Feder JN, Gnirke A, Thomas W, Tsuchihashi Z, Ruddy DA, Basava A, Dormishian F, Domingo R, Jr., Ellis MC, Fullan A, Hinton LM, Jones NL, Kimmel BE, Kronmal GS, Lauer P, Lee VK, Loeb DB, Mapa FA, McClelland E, Meyer NC, Mintier GA, Moeller N, Moore T, Morikang E, Prass CE, Quintana L, Starnes SM, Schatzman RC, Brunke KJ, Drayna DT, Risch NJ, Bacon BR, and Wolff RK. A novel MHC class I-like gene is mutated in patients with hereditary haemochromatosis. *Nat Genet* 13: 399–408, 1996.

11. Finberg KE, Whittlesey RL, and Andrews NC. Tmprss6 is a genetic modifier of the Hfe-hemochromatosis phenotype in mice. *Blood* 117: 4590–4599, 2011.

12. Fleming RE. Iron sensing as a partnership: HFE and transferrin receptor 2. *Cell Metab* 9: 211–212, 2009.

13. Ganz T. Hepcidin and iron regulation, 10 years later. *Blood* 117: 4425–4433, 2011.

14. Ganz T and Nemeth E. Hepcidin and disorders of iron metabolism. *Annu Rev Med* 62: 347–360, 2011.

15. Gao J, Chen J, Kramer M, Tsukamoto H, Zhang AS, and Enns CA. Interaction of the hereditary hemochromatosis protein HFE with transferrin receptor 2 is required for transferrin-induced hepcidin expression. *Cell Metab* 9: 217–227, 2009.

16. Hentze MW, Muckenthaler MU, Galy B, and Camaschella C. Two to tango: regulation of mammalian iron metabolism. *Cell* 142: 24–38, 2010.

17. Huang FW, Pinkus JL, Pinkus GS, Fleming MD, and Andrews NC. A mouse model of juvenile hemochromatosis. *J Clin Invest* 115: 2187–2191, 2005.

18. Jomova K and Valko M. Importance of iron chelation in free radical-induced oxidative stress and human disease. *Curr Pharm Des* 17: 3460–3473, 2011.

19. Kautz L, Meynard D, Besson-Fournier C, Darnaud V, Al Saati T, Coppin H, and Roth MP. BMP/Smad signaling is not enhanced in Hfe-deficient mice despite increased Bmp6 expression. *Blood* 114: 2515–2520, 2009.

20. Krause A, Neitz S, Magert HJ, Schulz A, Forssmann WG, Schulz-Knappe P, and Adermann K. LEAP-1, a novel highly disulfide-bonded human peptide, exhibits antimicrobial activity. *FEBS Lett* 480: 147–150, 2000.

21. Krijt J, Niederkofler V, Salie R, Sefc L, Pelichovska T, Vokurka M, and Necas E. Effect of phlebotomy on hepcidin expression in hemojuvelin-mutant mice. *Blood Cells Mol Dis* 39: 92–95, 2007.

22. Le Gac G, Scotet V, Ka C, Gourlaouen I, Bryckaert L, Jacolot S, Mura C, and Ferec C. The recently identified type 2A juvenile haemochromatosis gene (HJV), a second candidate modifier of the C282Y homozygous phenotype. *Hum Mol Genet* 13: 1913–1918, 2004.

23. Lebron JA, Bennett MJ, Vaughn DE, Chirino AJ, Snow PM, Mintier GA, Feder JN, and Bjorkman PJ. Crystal structure of the hemochromatosis protein HFE and characterization of its interaction with transferrin receptor. *Cell* 93: 111–123, 1998.

24. Lee P, Peng H, Gelbart T, Wang L, and Beutler E. Regulation of hepcidin transcription by interleukin-1 and interleukin-6. *Proc Natl Acad Sci U S A* 102: 1906–1910, 2005.

25. Nicolas G, Bennoun M, Devaux I, Beaumont C, Grandchamp B, Kahn A, and Vaulont S. Lack of hepcidin gene expression and severe tissue iron overload in upstream stimulatory factor 2 (USF2) knockout mice. *Proc Natl Acad Sci U S A* 98: 8780–8785, 2001.

26. Nili M, Shinde U, and Rotwein P. Soluble repulsive guidance molecule c/hemojuvelin is a broad spectrum bone morphogenetic protein (BMP) antagonist and inhibits both BMP2- and BMP6-mediated signaling and gene expression. *J Biol Chem* 285: 24783–24792, 2010.

27. Papanikolaou G, Samuels ME, Ludwig EH, MacDonald ML, Franchini PL, Dube MP, Andres L, MacFarlane J, Sakellaropoulos N, Politou M, Nemeth E, Thompson J, Risler JK, Zaborowska C, Babakaiff R, Radomski CC, Pape TD, Davidas O, Christakis J, Brissot P, Lockitch G, Ganz T, Hayden MR, and Goldberg YP. Mutations in HFE2 cause iron overload in chromosome 1q-linked juvenile hemochromatosis. *Nat Genet* 36: 77–82, 2004.

28. Poli M, Luscieti S, Gandini V, Maccarinelli F, Finazzi D, Silvestri L, Roetto A, and Arosio P. Transferrin receptor 2 and HFE regulate furin expression *via* mitogen-activated protein kinase/extracellular signal-regulated kinase (MAPK/Erk) signaling. Implications for transferrin-dependent hepcidin regulation. *Haematologica* 95: 1832–1840, 2010.

29. Ramey G, Deschemin JC, and Vaulont S. Cross-talk between the mitogen activated protein kinase and bone morphogenetic protein/hemojuvelin pathways is required for the induction of hepcidin by holotransferrin in primary mouse hepatocytes. *Haematologica* 94: 765–772, 2009.

30. Ramos E, Kautz L, Rodriguez R, Hansen M, Gabayan V, Ginzburg Y, Roth MP, Nemeth E, and Ganz T. Evidence for distinct pathways of hepcidin regulation by acute and chronic iron loading in mice. *Hepatology* 53: 1333–1341, 2011.

31. Roetto A, Papanikolaou G, Politou M, Alberti F, Girelli D, Christakis J, Loukopoulos D, and Camaschella C. Mutant antimicrobial peptide hepcidin is associated with severe juvenile hemochromatosis. *Nat Genet* 33: 21–22, 2003.

32. Schmidt PJ, Andrews NC, and Fleming MD. Hepcidin induction by transgenic overexpression of Hfe does not require the Hfe cytoplasmic tail, but does require hemojuvelin. *Blood* 116: 5679–5687, 2010.

33. Schmidt PJ, Toran PT, Giannetti AM, Bjorkman PJ, and Andrews NC. The transferrin receptor modulates Hfe-dependent regulation of hepcidin expression. *Cell Metab* 7: 205–214, 2008.

34. Torrance JD and Bothwell TH. Tissue iron stores. In: *Methods in Hematology: Iron,* edited by Cook JD. New York: Churchill Livingstone, 1980, pp. 90–115.

35. Truksa J, Peng H, Lee P, and Beutler E. Bone morphogenetic proteins 2, 4, and 9 stimulate murine hepcidin 1 expression independently of Hfe, transferrin receptor 2 (Tfr2), and IL-6. *Proc Natl Acad Sci U S A* 103: 10289–10293, 2006.

36. Verga Falzacappa MV, Vujic Spasic M, Kessler R, Stolte J, Hentze MW, and Muckenthaler MU. STAT3 mediates hepatic hepcidin expression and its inflammatory stimulation. *Blood* 109: 353–358, 2007.

37. Wallace DF, Summerville L, Crampton EM, Frazer DM, Anderson GJ, and Subramaniam VN. Combined deletion of Hfe and transferrin receptor 2 in mice leads to marked dysregulation of hepcidin and iron overload. *Hepatology* 50: 1992–2000, 2009.

38. Wang Q, Jiang L, Wang J, Li S, Yu Y, You J, Zeng R, Gao X, Rui L, Li W, and Liu Y. Abrogation of hepatic ATP-citrate lyase protects against fatty liver and ameliorates hyperglycemia in leptin receptor-deficient mice. *Hepatology* 49: 1166–1175, 2009.

39. Zhang Z, Zhang F, An P, Guo X, Shen Y, Tao Y, Wu Q, Zhang Y, Yu Y, Ning B, Nie G, Knutson MD, Anderson GJ, and Wang F. Ferroportin1 deficiency in mouse macrophages impairs iron homeostasis and inflammatory responses. *Blood* 118: 1912–1922, 2011.

40. Zhang Z, Zhang F, Guo X, An P, Tao Y, and Wang F. Ferroportin1 in hepatocytes and macrophages is required for the efficient mobilization of body iron stores in mice. *Hepatology* 56: 961–971, 2012.

41. Zhou XY, Tomatsu S, Fleming RE, Parkkila S, Waheed A, Jiang J, Fei Y, Brunt EM, Ruddy DA, Prass CE, Schatzman RC, O'Neill R, Britton RS, Bacon BR, and Sly WS. HFE gene knockout produces mouse model of hereditary hemochromatosis. *Proc Natl Acad Sci U S A* 95: 2492–2497, 1998.

Address correspondence to:
Dr. Fudi Wang
Department of Nutrition
Research Center for Nutrition and Health
Institute of Nutrition and Food Safety
School of Public Health
School of Medicine
Zhejiang University
Hangzhou 310058
China

E-mail: fwang@zju.edu.cn
fudiwang.lab@gmail.com

Dr. Junxia Min
The First Affiliated Hospital
Institute for Translational Medicine
School of Medicine
Zhejiang University
Hangzhou 310058
China

E-mail: junxiamin@zju.edu.cn

Abbreviations Used

ANOVA = analysis of variance
BMP = bone morphogenetic protein
DID = dietary-induced iron deficiency
Erk = extracellular signal regulated kinase
Fpn1 = ferroportin1
HAMP1 = hepcidin antimicrobial peptide 1
HFE = hemochromatosis protein
HH = hereditary hemochromatosis
HIC = hepatic iron content

HJV = hemojuvelin
MAPK = mitogen-activated protein kinase
PCR = polymerase chain reaction
P-Erk = phosphorylated Erk
P-SMAD1/5/8 = phosphorylated Smad1/5/8
RBC = red blood cell
RT-PCR = reverse transcription polymerase chain reaction
SMAD = mothers against decapentaplegic homolog proteins
STAT3 = signal transducers and activators of transcription 3
Tf = transferrin
TfR1 = transferrin receptor 1
TfR2 = transferrin receptor 2
WT = wild-type